Theory for Ligand Rebinding at Cell Membrane Surfaces

B. Christoffer Lagerholm and Nancy L. Thompson
Department of Chemistry, University of North Carolina, Chapel Hill, North Carolina 27599-3290 USA

ABSTRACT Conditions for which a ligand reversibly bound to a cell surface dissociates and then rebinds to the surface have been theoretically examined. The coupled differential equations that describe reaction at the interface between sites on a plane and three-dimensional solution have been described previously (Thompson, N. L., T. P. Burghardt, and D. Axelrod. 1981. *Biophys. J.* 33:435–454). Here, we use this theoretical formalism to provide an analytical solution for the spatial and temporal dependence of the probabilities of finding a molecule on the surface or in the solution, given initial placement on the surface at the origin. This general analytical solution is used to derive a simple expression for the probability that a molecule rebinds to the surface at a given position and time after release at the origin and time zero. The probability expressions provide fundamental equations that form a basis for subsequent modeling of ligand-receptor interactions in specific geometries.

INTRODUCTION

Numerous biochemical processes are mediated by interactions between soluble ligands and cell-surface receptors. Considerable effort has been devoted to understanding the role of ligand-receptor interactions in the mechanisms of these processes. A series of theoretical investigations into the thermodynamic, kinetic, and transport characteristics of interactions between macromolecules in three-dimensional solution and sites on a planar or spherical surface has been presented (e.g., Adam and Delbrück, 1968; Berg and Purcell, 1977; DeLisi and Wiegel, 1981; Shoup and Szabo, 1982; Berg and von Hippel, 1985; Northrup et al., 1986; Northrup, 1988; Zwanzig, 1990; Wang et al., 1992; Axelrod and Wang, 1994; Forsten and Lauffenburger, 1994; Lauffenburger et al., 1995; Goldstein and Dembo, 1995; Balgi et al., 1995; Model and Omann, 1995). These investigations have suggested that a phenomenon of particular importance is the process in which reversibly bound ligands dissociate from receptors, diffuse for a time in the nearby solution, and then rebind to the same or a nearby receptor on the cell surface. Evidence for the rebinding process has been experimentally obtained for a variety of ligand-receptor systems, including haptens with IgE-coated mast cells (Erickson et al., 1987; Goldstein et al., 1989; Erickson et al., 1991); bovine prothrombin fragment 1 with negatively charged substrate-supported planar membranes (Pearce et al., 1992); antibodies with immobilized peptides (Duschl et al., 1996); lipoprotein lipase with immobilized heparin sulfate (Lookene et al., 1996); and neurotransmitters in synapses (Otis et al., 1996).

In this work, a rigorous theoretical treatment of the rebinding process is presented. An analytical solution for the spatial and temporal dependence of the probabilities of finding the molecule on the surface or in the solution, given initial placement at the origin, is derived. This general analytical solution is used to find a simple expression for the probability that a molecule rebinds to the surface at a given position and time, after initial release (not placement) at the origin. The probability expressions provide fundamental equations forming the basis for subsequent modeling of ligand-receptor interactions in particular geometries.

RESULTS

General considerations

Consider a reversible bimolecular reaction at a surface (the *xy*-plane) coupled with diffusion in solution (Fig. 1). A concentration of molecules in solution, A, is in equilibrium with a density of molecules on the surface, C, and a density of unoccupied, immobile surface binding sites, B. We imagine a case where a tagged molecule is placed on the surface, at the origin, at time zero. The system remains in chemical equilibrium while the tagged molecule explores the surface and solution with time. The reaction mechanism may be written as

$$A + B \underset{k_d}{\overset{k_a}{\rightleftarrows}} C \tag{1}$$

where k_a and k_d are the kinetic association and dissociation rate constants, respectively. Of interest are the probabilities $P_C(x, y, t)$ and $P_A(x, y, z, t)$ for finding the tagged molecule on the surface or in solution, respectively, at time $t > 0$. These functions may be used to calculate parameters that describe rebinding of the tagged molecule at the surface.

Received for publication 26 June 1997 and in final form 25 November 1997.

Address reprint requests to Dr. Nancy L. Thompson, Department of Chemistry, University of North Carolina, CB-3290, Chapel Hill, NC 27599-3290. Tel.: 919-962-0328; Fax: 919-962-2388; E-mail: nlt@unc.edu.

0006-3495/98/03/1215/14 $2.00

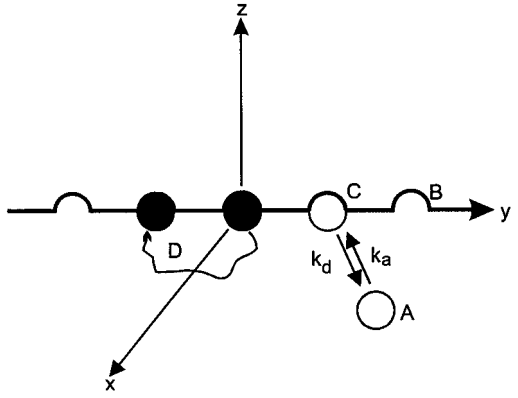

FIGURE 1 Schematic of rebinding phenomenon. Molecules in solution (*open circle*) (*A*) are in equilibrium with free surface binding sites (*B*) and occupied surface binding sites (*C*). The association and dissociation rate constants are k_a and k_d, respectively. A single tagged molecule (*closed circle*) is placed at the origin at time zero. As time proceeds, the tagged molecule dissociates from the surface, explores the solution with diffusion coefficient *D*, and rebinds to the surface at a different position and later time.

Differential equations

We begin with the differential equations that govern the reaction:

$$\frac{\partial}{\partial t}P_C(x, y, t) = k_a B[P_A(x, y, z, t)]_{z=0} - k_d P_C(x, y, t) \tag{2}$$

$$\frac{\partial}{\partial t}P_A(x, y, z, t) = D\nabla^2 P_A(x, y, z, t) \tag{3}$$

where D is the diffusion coefficient of the tagged molecule in solution and ∇^2 is the three-dimensional Laplacian. Because the system is in chemical equilibrium, the density of free surface sites, B, the concentration of molecules in solution A, and the density of bound molecules, C, are constant and the differential equations are linear rather than nonlinear.

Initial and boundary conditions

At time zero, we define the probability of locating the molecule on the surface by a normal distribution around the origin with a small width, a, and the probability of finding the molecule in solution as zero:

$$[P_C(x, y, t)]_{t=0} = \frac{1}{\pi a^2}\exp\left[-\frac{(x^2 + y^2)}{a^2}\right]$$
$$[P_A(x, y, z, t)]_{t=0} = 0 \tag{4}$$

As $a \to 0$, the initial surface probability is a Dirac delta function located at the origin. Nine of the ten required boundary conditions are

$$[P_C(x, y, t)]_{x,y=\pm\infty} = 0$$
$$[P_A(x, y, z, t)]_{x,y=\pm\infty,z=\infty} = 0 \tag{5}$$

The final boundary condition describes the flux at the surface:

$$D\left[\frac{\partial}{\partial z}P_A(x, y, z, t)\right]_{z=0} = k_a B[P_A(x, y, z, t)]_{z=0} - k_d P_C(x, y, t) \tag{6}$$

General solutions for $P_C(r, t)$ and $P_A(r, z, t)$

To describe the rebinding process, we have analytically solved the set of equations given above (Eqs. 2–6) for the surface density probability and the solution concentration probability. The details are given in Appendix A. The expressions for $P_C(r, t)$ and $P_A(r, z, t)$, where $\mathbf{r} = (x, y)$, are

$$P_C(r, t) = \frac{1}{2\pi}\int_0^\infty \exp\left[-q^2\left(Dt + \frac{a^2}{4}\right)\right] \cdot J_0(qr)\sum_{i=1}^{3} f_i w[-i\sqrt{\alpha_i t}]q\, dq \tag{7}$$

$$P_A(r, z, t) = \frac{1}{2\pi}\frac{k_d}{\sqrt{D}}\int_0^\infty \exp\left[-q^2\left(Dt + \frac{a^2}{4}\right) - \frac{z^2}{4Dt}\right] \cdot J_0(qr)\sum_{i=1}^{3}\frac{f_i}{\sqrt{\alpha_i} + \beta} w\left[i\left(\frac{z}{\sqrt{4Dt}} - \sqrt{\alpha_i t}\right)\right]q\, dq \tag{8}$$

In these equations, q is an integration variable that results from a Fourier transform with $\mathbf{r} \to \mathbf{q}$, $J_0(qr)$ is the zero-order Bessel function, and the w function is defined as (Abramowitz and Stegun, 1974)

$$w[\xi] = \exp[-\xi^2]\mathrm{erfc}[-i\xi] \tag{9}$$

The rates α_i, and the fractional amplitudes f_i, of the three terms containing w functions with arguments dependent on the α_i, are given by

$$\alpha_i^{3/2} + \beta\alpha_i + (k_d - Dq^2)\alpha_i^{1/2} - \beta Dq^2 = 0 \tag{10}$$

$$f_i = \frac{\sqrt{\alpha_i}(\sqrt{\alpha_i} + \beta)}{(\sqrt{\alpha_i} - \sqrt{\alpha_j})(\sqrt{\alpha_i} - \sqrt{\alpha_k})} \qquad \beta = \frac{k_a B}{\sqrt{D}} \tag{11}$$

where $i \neq j \neq k$. The expressions shown in Eq. 7 and Eqs. 9–11 are similar to those derived previously in a different context (Thompson et al., 1981).

Characteristic rates and distances

It is instructive to write $P_C(r, t)$ and $P_A(r, z, t)$ in terms of physically significant characteristic rates and distances whose relative sizes determine the shapes of these functions. The resulting expressions are also useful for generating more concise plots of $P_C(r, t)$ and $P_A(r, z, t)$ (see below). One characteristic rate is the surface dissociation rate, k_d. Another characteristic rate is

$$k_t = D\left(\frac{k_d}{k_a B}\right)^2 = \frac{D}{N^2}(K_d + A)^2 \quad K_d = \frac{k_d}{k_a} \tag{12}$$

In Eq. 12, N is the total density of surface binding sites (occupied and unoccupied) and K_d is the equilibrium dissociation constant. A characteristic length may be found by using the solution diffusion coefficient and the intrinsic dissociation rate. This length is defined as

$$\gamma = \sqrt{\frac{D}{k_d}} \tag{13}$$

Dimensionless forms of the probability functions

By writing the time and lengths in dimensionless forms as

$$\tau = k_d t \quad \rho = \frac{r}{\gamma} \quad \eta = \frac{z}{\gamma} \quad \kappa = \frac{a}{\gamma} \tag{14}$$

the probability expressions may be written in dimensionless form as

$$Q_C(\rho, \tau) = \gamma^2 P_C(\rho, \tau)$$
$$= \frac{1}{2\pi}\int_0^\infty \exp\left[-c^2\left(\tau + \frac{\kappa^2}{4}\right)\right] J_0(c\rho) \sum_{i=1}^{3} f_i w[-iu_i\sqrt{\tau}]c\, dc \tag{15}$$

$$Q_A(\rho, \eta, \tau) = \gamma^3 P_A(\rho, \eta, \tau)$$
$$= \frac{1}{2\pi}\int_0^\infty \exp\left[-c^2\left(\tau + \frac{\kappa^2}{4}\right) - \frac{\eta^2}{4\tau}\right] \tag{16}$$
$$\cdot J_0(c\rho) \sum_{i=1}^{3} \frac{f_i}{u_i + b} w\left[i\left(-u_i\sqrt{\tau} + \frac{\eta}{2\sqrt{\tau}}\right)\right] c\, dc$$

The parameter c is a dimensionless integration variable, and

$$u_i^3 + bu_i^2 + (1 - c^2)u_i - bc^2 = 0 \tag{17}$$

$$f_i = \frac{u_i(u_i + b)}{(u_i - u_j)(u_i - u_k)} \quad b = \sqrt{\frac{k_d}{k_t}} \tag{18}$$

The parameter b

If the time t is cast as a product with k_d, and the lengths r, z, and a are scaled by the length γ, then the shape of the dimensionless probability densities, $Q_C(\rho, \tau)$ and $Q_A(\rho, \eta, \tau)$ (Eqs. 15 and 16), written in terms of the dimensionless variables, is entirely determined by the parameters κ and b, where (see Eqs. 12 and 18)

$$b = \frac{k_a N}{k_d + k_a A}\sqrt{\frac{k_d}{D}} \tag{19}$$

Typical values of the parameter b for various experimentally relevant conditions are shown in Fig. 2.

The parameter b is interpreted as a measure of the likelihood of prompt rebinding. For example, if N approaches zero or D approaches infinity, the parameter b approaches zero. In these limits, rebinding does not occur either because

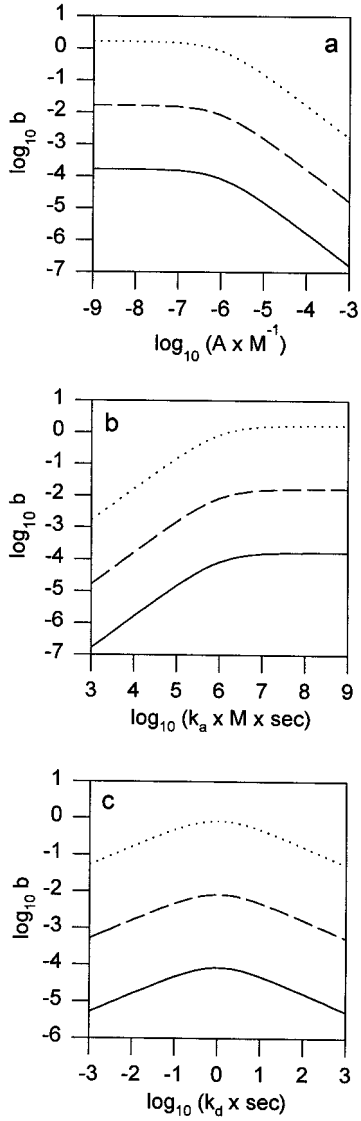

FIGURE 2 Typical values of the rebinding parameter b. The values of the rebinding parameter b are shown as a function of (*a*) the solution concentration, A, (*b*) the association rate, k_a, and (*c*) the dissociation rate, k_d. For all plots, the solution diffusion coefficient D equals 10^{-6} cm^2s^{-1} and the total surface site density $N = 1$ molecule/μm^2 (*line*), 10^2 molecules/μm^2 (*dash*), or 10^4 molecules/μm^2 (*dot*). In (*a*), $k_a = 10^6$ $M^{-1}s^{-1}$ and $k_d = 1$ s^{-1}. In (*b*), $A = 10^{-6}$ M and $k_d = 1$ s^{-1}. In (*c*), $k_a = 10^6$ M^{-1} s^{-1} and $A = 10^{-6}$ M. Values were calculated using Eq. 19.

there are no surface binding sites available for occupation by the tagged molecule, or because the tagged molecule quickly diffuses away from the surface before rebinding. On the other hand, if N approaches infinity or D approaches zero, rebinding is promoted and the parameter b approaches infinity.

The parameter b depends in a more complex manner on the solution concentration A than on D and N. As the concentration of untagged molecules in solution is increased, the surface density C is increased, rebinding is blocked and b decreases to zero. In this case, untagged molecules in solution compete with the tagged molecule for surface binding sites. At low solution concentrations A, b equals a limiting value given by

$$b' = \frac{k_a N}{\sqrt{D k_d}} \tag{20}$$

In this limit, even though very few of the surface binding sites are occupied, b does not become infinitely large. The parameter b' describes the extent of rebinding in the case where competition from solution phase molecules is negligible.

The dependence of the parameter b on the association rate constant k_a is also nonlinear. As k_a is decreased, b decreases to zero. This limit describes the case in which the surface acts as a reflecting wall. When the constant k_a is increased to infinity, the parameter b reaches a limiting value given by

$$b'' = \sqrt{\frac{k_d}{D}}\frac{N}{A} \tag{21}$$

The parameter b'', which does approach infinity if the solution concentration is zero, can be understood as describing the extent of rebinding when the association rate constant is high but the surface binding sites are partially occupied.

The dependence of the parameter b on the dissociation rate constant k_d is somewhat complex. The limit of no rebinding, $b \to 0$, is reached if k_d approaches either zero or infinity. When k_d is very large, the surface acts as a reflecting wall. When k_d is very small, the equilibrium dissociation constant is small, binding of untagged ligands is promoted, and the surface binding sites to which the tagged molecule might rebind are blocked. As a function of k_d, the parameter b peaks when

$$k_d = k_a A \qquad b = \frac{1}{2}\sqrt{\frac{k_d}{D}}\frac{N}{A} = \frac{1}{2}b'' \tag{22}$$

This condition is the one in which the surface binding sites are half-occupied. In this case, the extent of rebinding is maximized by balancing the inhibitive effects of low and high kinetic dissociation constants.

It is instructive to write the parameter b in terms of the density of occupied surface binding sites, the solution concentration, and the length γ, i.e.,

$$b = \frac{C}{A}\frac{1}{\gamma} \qquad \frac{C}{A} = \frac{N}{K_d + A} \tag{23}$$

As shown, b is the ratio of two lengths. The first length, C/A, is the thickness of a slab in solution that contains a density of untagged molecules equal to the density of untagged molecules on the surface. The second length, γ (Eq. 13), is the average distance traveled by diffusion in solution during the average surface residency time, k_d^{-1}. If $\gamma \gg C/A$, the molecule diffuses away from the surface and rebinding is not favored. On the other hand, if $\gamma \ll C/A$, diffusion in solution is comparatively slow, and rebinding is favored. Fig. 3 *a* shows the values of the characteristic length γ as a function of the dissociation rate k_d, and Figs. 3 *b* and *c* show the values of the length C/A for typical values of N, K_d, and A.

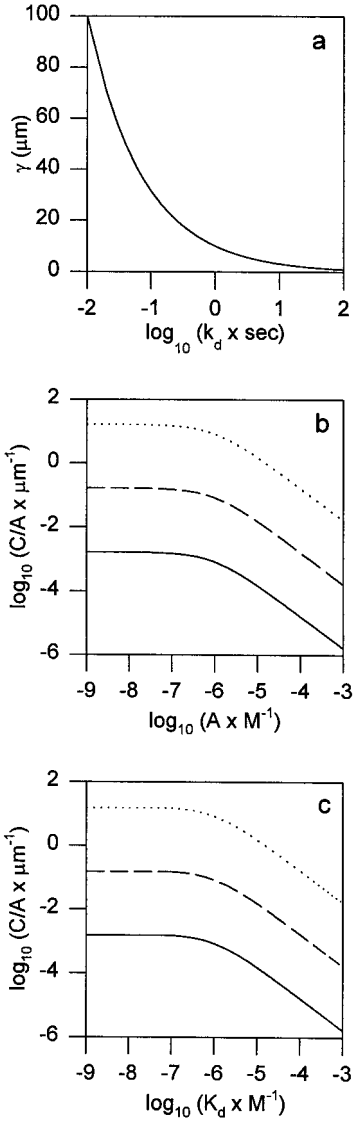

FIGURE 3 Typical values for the characteristic lengths γ and C/A. In (*a*), the values of the length γ (Eq. 13) are shown as a function of the dissociation rate, k_d, with the solution diffusion coefficient, D, equal to 10^{-6} cm^{2}s^{-1}. Also shown are the values of the length C/A (Eq. 23), where C is the surface density, as a function of (*b*) the solution concentration, A, and (*c*) the equilibrium dissociation constant, K_d. In (*b*) and (*c*), the total surface site density, N, equals 1 molecule/μm^2 (*line*), 10^2 molecules/μm^2 (*dash*) or 10^4 molecules/μm^2 (*dot*). In (*b*), $K_d = 10^{-6}$ M. In (*c*), $A = 10^{-6}$ M.

Limiting solutions for $P_C(r, t)$ and $P_A(r, z, t)$

A closed form solution may be obtained for $P_C(r, t)$ in the limit of no rebinding ($b \to 0$). In this case (Eqs. 17 and 18),

$$u_{1,2} = \pm\sqrt{c^2 - 1} \qquad u_3 = 0$$
$$f_{1,2} = 1/2 \qquad f_3 = 0 \tag{24}$$

By using these values in Eqs. 7 and 15, one finds that (Abramowitz and Stegun, 1974)

$$Q_C(\rho, \tau) = \frac{1}{\pi\kappa^2}\exp\left[-\tau - \frac{\rho^2}{\kappa^2}\right]$$
$$P_C(r, t) = \frac{1}{\pi a^2}\exp\left[-k_d t - \frac{r^2}{a^2}\right] \tag{25}$$

In this limit, the tagged molecule dissociates from its initial binding site near the origin in an exponential fashion with rate k_d, and is never again found on the surface.

In the limit of infinite rebinding, $b \to \infty$, simple forms for both $P_C(r, t)$ and $P_A(r, z, t)$ can be found. In this case (Eqs. 17 and 18)

$$u_{1,2} \approx \pm c \mp 1/(2b) \qquad u_3 \approx -b$$
$$f_{1,2} \approx 1/2 \qquad f_3 \approx 0 \tag{26}$$

By using these values in Eqs. 7, 8, 15, and 16, one finds that

$$Q_C(\rho, \tau) \approx \frac{1}{\pi\kappa^2}\exp\left[-\frac{\rho^2}{\kappa^2}\right]$$
$$P_C(r, t) \approx \frac{1}{\pi a^2}\exp\left[-\frac{r^2}{a^2}\right] \tag{27}$$

$$Q_A(\rho, \eta, \tau) \approx 0 \quad P_A(r, z, t) \approx 0 \tag{28}$$

In this limit, the tagged molecule remains bound at the origin and is never found in the solution.

Plots of the general solutions for $Q_C(\rho, \tau)$ and $Q_A(\rho, \eta, \tau)$

The surface probability density $Q_C(\rho, \tau)$ and the solution probability density $Q_A(\rho, \eta, \tau)$ can be calculated by numerical integration of Eqs. 15 and 16. Figs. 4–6 show the results of these calculations for four values of the rebinding parameter b (0.01, 1, 100, 10^4). Two values of the parameter κ are considered, which correspond to $a = 30$ Å and $D = 10^{-6}$ cm^{2}s^{-1}. In the first set of plots, the intrinsic surface dissociation constant is large ($k_d = 100$ s^{-1}), the characteristic length γ is small ($\gamma = 1$ μm), and $\kappa = 3 \times 10^{-3}$. In the

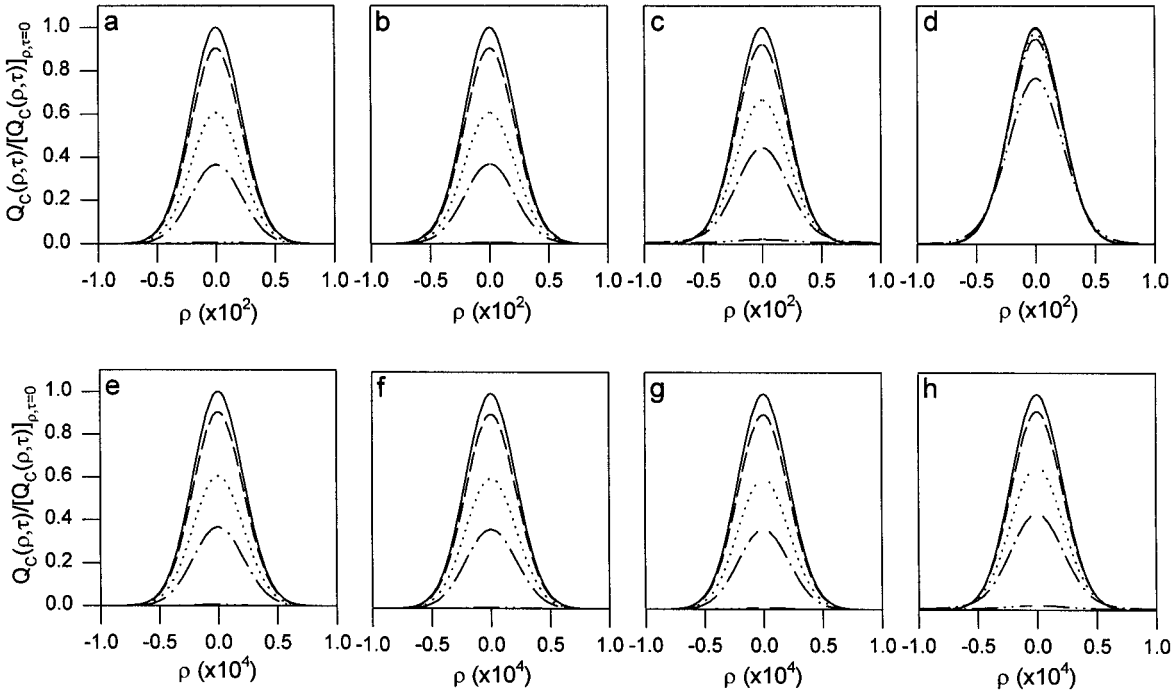

FIGURE 4 Surface density probability, $Q_C(\rho, \tau)$, near the origin. $P_C(r, t) = (D/k_d)\,Q_C(\rho, \tau)$ is the probability density of finding a tagged molecule at the surface at position r and time t, given the distribution at time zero from Eq. 4, where k_d is the surface dissociation rate, ρ is a dimensionless form of the surface position, and τ is a dimensionless form of the time (Eqs. 13 and 14). $Q_C(\rho, \tau)$ was calculated by numerical integration of Eq. 15, for a particle radius, a, of 30 Å, and a solution diffusion coefficient, D, of 10^{-6} cm^{2}s^{-1}. In (*a–d*), $k_d = 100$ s^{-1}, implying $\gamma = 1$ μm and $\kappa = 3 \times 10^{-3}$, and in (*e–h*) $k_d = 0.01$ s^{-1}, implying $\gamma = 100$ μm and $\kappa = 3 \times 10^{-5}$ (Eqs. 13 and 14). The rebinding parameter b (Eq. 19, Fig. 2) equals (*a* and *e*) 0.01, (*b* and *f*) 1, (*c* and *g*) 100, or (*d* and *h*) 10^4. The probability density was plotted for τ equal to 0 (*line*), 0.1 (*dash*), 0.5 (*dot*), 1 (*dot-dash*), and 5 (*dot-dot-dash*). The surface density probability, $Q_C(\rho, \tau)$, was normalized by the surface density probability at the origin at time zero, $[Q_C(\rho, \tau)]_{\rho,\tau=0}$.

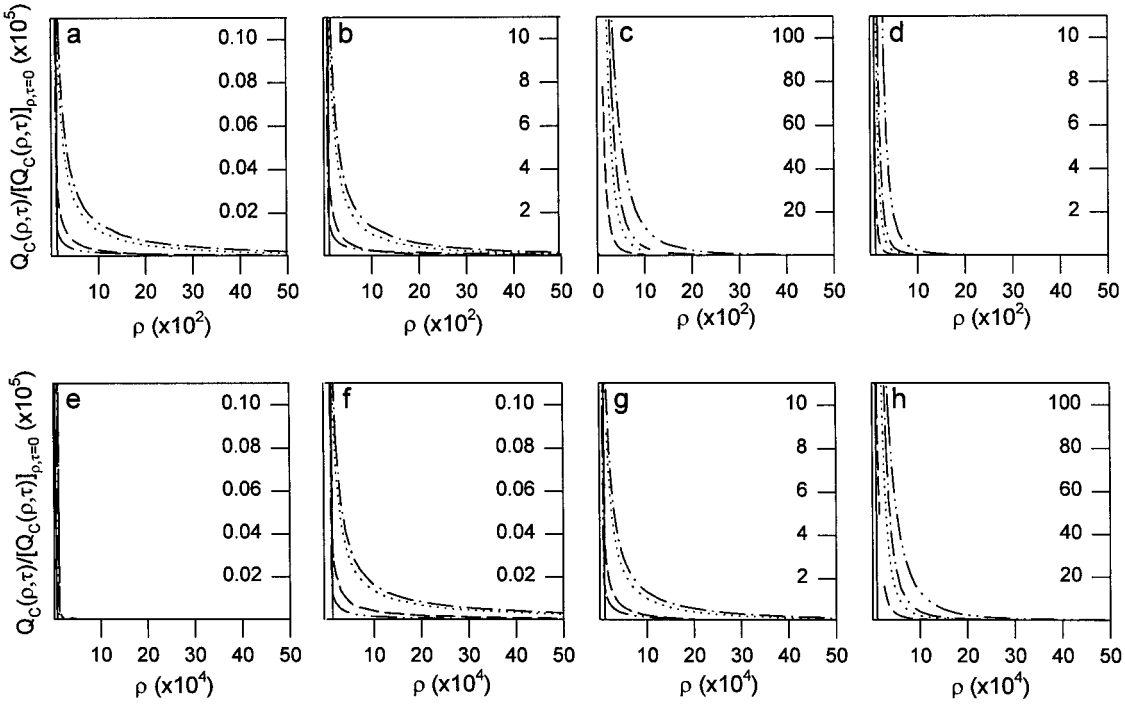

FIGURE 5 Surface density probability, $Q_C(\rho, \tau)$, far from the origin. $P_C(r, t) = (D/k_d)\, Q_C(\rho, \tau)$ is the probability density of finding a tagged molecule at the surface at position r and time t, given the distribution at time zero from Eq. 4, where k_d is the surface dissociation rate, ρ is a dimensionless form of the surface position, and τ is a dimensionless form of the time (Eqs. 13 and 14). $Q_C(\rho, \tau)$ was calculated by numerical integration of Eq. 15, for a particle radius, a, of 30 Å, and a solution diffusion coefficient, D, of 10^{-6} cm^{2}s^{-1}. In (*a–d*), $k_d = 100$ s^{-1}, implying $\gamma = 1$ μm and $\kappa = 3 \times 10^{-3}$, and in (*e–h*) $k_d = 0.01$ s^{-1}, implying $\gamma = 100$ μm and $\kappa = 3 \times 10^{-5}$ (Eqs. 13 and 14). The rebinding parameter b (Eq. 19, Fig. 2) equals (*a* and *e*) 0.01, (*b* and *f*) 1, (*c* and *g*) 100, or (*d* and *h*) 10^4. The probability density was plotted for τ equal to 0 (*line*), 0.1 (*dash*), 0.5 (*dot*), 1 (*dot-dash*), and 5 (*dot-dot-dash*). The surface density probability, $Q_C(\rho, \tau)$, was normalized by the surface density probability at the origin at time zero, $[Q_C(\rho, \tau)]_{\rho,\tau=0}$.

second set, the dissociation constant is small ($k_d = 0.01$ s^{-1}), the length γ is large ($\gamma = 100$ μm), and $\kappa = 3 \times 10^{-5}$.

At time zero, the surface probability function $Q_C(\rho, \tau)$ is a spatial Gaussian with width κ (Eq. 4). Near the origin, this Gaussian shape is retained approximately as time proceeds (Fig. 4). The primary feature in this spatial region is that the peak at $\rho = 0$ decreases in magnitude with time τ. For low values of b, this decrease is exponential in τ (Eq. 25) and reflects the desorption, without rebinding, of the molecule from its initial position on the surface. For higher values of b, the peak decreases more slowly with τ. This characteristic describes dissociation followed by rebinding at the same or a nearby position.

The behavior of the surface probability function is more complex further from the origin. Fig. 5 shows the values of $Q_C(\rho, \tau)$ for values of $\rho \approx 100\ \kappa$ (or $r \approx 100\ a = 0.3$ μm). At these positions, the probability (as plotted) that the molecule has been present at a given position since the initial time is given by (Eq. 25) $Q_C(\rho, \tau)/[Q_C(\rho, \tau)]_{\rho,\tau=0} \approx \exp[-\tau]\ \exp[-10^4]$. However, the magnitudes of $Q_C(\rho, \tau)/[Q_C(\rho, \tau)]_{\rho,\tau=0}$ are much larger, on the order of 10^{-9} to 10^{-3}. Therefore, these relatively high values of the surface probability functions represent the probability that the molecule has dissociated and rebound to the surface.

For small values of b (Fig. 5, *a*, *e*, and *f*), at large values of ρ, the probability of rebinding after a given time is very small. For larger values of b (Fig. 5, *b*, *c*, *g*, and *h*), molecules travel large distances in solution before rebinding, resulting in a spread of molecules away from the origin. In the case of even larger values of b (Fig. 5 *d*), the higher probability of rebinding after a short time results in slower spread as molecules rebind closer to the origin. At very large values of b, rebinding occurs at, or very near, the origin as the probability of a molecule being in the solution approaches zero. In this case there is very little spread of molecules along the surface. The maximum spread occurs at large values of b for smaller values of κ (Fig. 5, *c* and *h*). A final feature (apparent in Fig. 5, *a*, *b*, *f*, and *g*) is that, at a given position, the surface probability increases, peaks, and then decreases with time. This feature results from the combination of increased spreading at larger times along with a lower probability of finding the molecule anywhere on the surface at these later times.

The plots for the solution probability, $Q_A(\rho, \eta, \tau)$, (Fig. 6) demonstrate the b-dependence of rebinding well. The solution concentration is at a maximum for lower values of b, while it approaches zero as b becomes very large. Furthermore, it is demonstrated that once a molecule is in the solution it rapidly diffuses away from the surface so that for longer times, τ, there is a very low probability that the molecule is in solution next to the surface. For larger values of b, the molecule rebinds faster than it diffuses away in

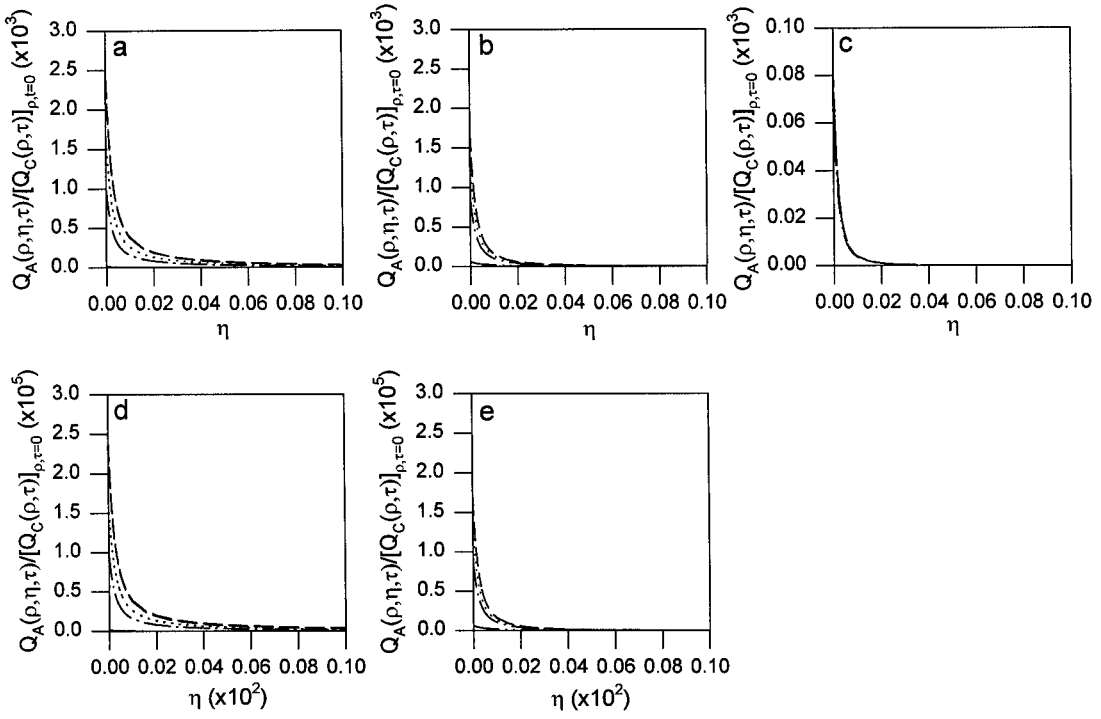

FIGURE 6 Solution probability $Q_A(\rho, \eta, \tau)$. $P_A(r, z, t) = (D/k_d)^{3/2}\, Q_A(\rho, \eta, \tau)$ is the probability of finding the tagged molecule in solution a distance r from the origin and a distance z from the surface, at time t, where k_d is the surface dissociation rate, ρ is a dimensionless form of the surface position, η is a dimensionless form of the distance from the surface, and τ is a dimensionless form of the time (Eqs. 13 and 14). $Q_A(\rho, \eta, \tau)$ was calculated by numerical integration of Eq. 16, for a particle radius, a, of 30 Å and a solution diffusion coefficient, D, of 10^{-6} cm^{2}s^{-1}. In (a–c) $k_d = 100$ s^{-1}, implying $\gamma = 1$ μm and $\kappa = 3 \times 10^{-3}$, and in ($d$ and e) $k_d = 0.01$ s^{-1}, implying $\gamma = 100$ μm and $\kappa = 3 \times 10^{-5}$ (Eqs. 13 and 14). The rebinding parameter b (Eq. 19, Fig. 2) equals (a and d) 0.01, (a and d) 1, (b and d) 100, or (c and e) 10^4. The probability density was plotted for τ equal to 0.1 (*dash*), 0.5 (*dot*), 1 (*dot-dash*), and 5 (*dot-dot-dash*). The solution probability was equivalent within plot resolution for (a) $k_d = 100$ s^{-1} and $b = 0.01$ or $b = 1$, and for (d) $k_d = 0.01$ s^{-1} and $b = 0.01$, $b = 1$, or $b = 100$. The solution probability, $Q_A(\rho, \eta, \tau)$, was normalized by the surface density probability at the origin at time zero, $[Q_C(\rho, \tau)]_{\rho,\tau=0}$.

solution, again illustrating the low spread of molecules along the surface at large b.

Spatially integrated surface probability $S(\tau)$

The probability of locating a molecule anywhere on the surface at time τ is found by integrating $Q_C(\rho, \tau)$ over all space:

$$S(\tau) = \int Q_C(\rho, \tau) d^2\rho = \sum_{i=1}^{3} [f_i w(-iu_i \sqrt{\tau}]_{c=0}$$

$$S(\tau) = \frac{a_2 w[-ia_1\sqrt{\tau}] - a_1 w[-ia_2\sqrt{\tau}]}{a_2 - a_1} \qquad (29)$$

$$a_{1,2} = -\frac{b}{2} \pm \sqrt{\frac{b^2}{4} - 1}$$

In the limit of no rebinding, $b \to 0$, and the spatial integral gives a simple exponential with rate k_d; in the limit of extreme rebinding, $b \to \infty$, and the spatial integral gives a w function with rate k_t (Abramowitz and Stegun, 1974):

$$[S(\tau)]_{b=0} = \exp[-\tau] = \exp[-k_d t]$$
$$[S(\tau)]_{b=\infty} = w\left[i\sqrt{\frac{\tau}{b^2}}\right] = w[i\sqrt{k_t t}] \to 1 \qquad (30)$$

The function $S(\tau)$ is shown in Fig. 7 and has been previously described (Thompson et al., 1981).

Temporal rebinding probability $Y(\tau)$

The function $S(\tau)$ describes the overall probability of finding the tagged molecule on the surface at time τ. Of interest also is the individual probability that a molecule rebinds at time τ, given initial release at time zero. This individual rebinding probability, $Y(\tau)$, can be found by writing $S(\tau)$ as an infinite sum of functions $S_n(\tau)$

$$S(\tau) = S_1(\tau) + S_2(\tau) + S_3(\tau) + \cdots \qquad (31)$$

where each successive population represents one additional dissociation and rebinding event. $S_1(\tau)$ is the probability that the tagged molecule has not yet dissociated at time τ. $S_2(\tau)$ is the probability that the molecule dissociated at time τ_1,

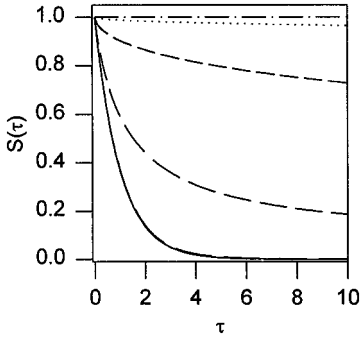

FIGURE 7 Spatially integrated surface probability $S(\tau)$. The function $S(\tau)$ gives the probability of finding the tagged molecule on the surface at time $t = \tau/k_d$, where k_d is the surface dissociation rate. This plot shows $S(\tau)$ as calculated from Eq. 29 for the rebinding parameter b equal to 0 (*line*), 0.01 (*long dash*), 1 (*intermediate dash*), 10 (*short dash*), 100 (*dot*), and ∞ (*dot-dash*).

rebound at time τ_2, and remains bound at time τ; averaged over all possible values of τ_1 and τ_2. $S_3(\tau)$ is the probability that the molecule dissociated at time τ_1, rebound at time τ_2, dissociated at time τ_3, rebound at time τ_4, and remains bound at time τ; averaged over all possible values of τ_1, τ_2, τ_3, and τ_4. Subsequent functions $S_n(\tau)$ are found by adding more dissociation and rebinding events.

The functions $S_n(\tau)$ are

$$S_1(\tau) = \exp[-\tau]$$

$$S_2(\tau) = \int_0^{\tau} d\tau_2 \int_0^{\tau_2} d\tau_1 \exp[-\tau_1] Y(\tau_2 - \tau_1)\exp[\tau_2 - \tau] \tag{32}$$

$$S_3(\tau) = \int_0^{\tau} d\tau_4 \int_0^{\tau_4} d\tau_3 \int_0^{\tau_3} d\tau_2 \int_0^{\tau_2} d\tau_1 \exp[-\tau_1]$$

$$\cdot Y(\tau_2 - \tau_1)\exp[\tau_2 - \tau_3] Y(\tau_4 - \tau_3)\exp[\tau_4 - \tau]$$

and so forth. $Y(\tau)$ is the probability that the molecule rebinds to the surface at time τ given initial release at time zero and is the function of interest. In the limit of no rebinding, $Y(\tau) = 0$, $S_n(\tau) = 0$ for $n \geq 2$, and

$$S(\tau) = \exp[-\tau] \tag{33}$$

In the limit of extreme rebinding, $Y(\tau) = \delta(\tau)$, and

$$S_2(\tau) = \tau \exp[-\tau]$$

$$S_3(\tau) = \frac{\tau^2}{2!} \exp[-\tau]$$

$$S_4(\tau) = \frac{\tau^3}{3!} \exp[-\tau] \tag{34}$$

$$S(\tau) = \left(1 + \tau + \frac{\tau^2}{2!} + \frac{\tau^3}{3!} + \cdots\right)$$

$$\cdot \exp[-\tau] = 1$$

These limits are consistent with Eqs. 30 (Fig. 7).

As shown in Appendix B, the function $Y(\tau)$ can be found by Laplace transforming $S(\tau)$ along with the $S_n(\tau)$, carrying out the infinite sum (Eq. 31) in Laplace transform space, and then inverse Laplace transforming. The simple result is

$$Y(\tau) = \frac{b}{\sqrt{\pi\tau}} - b^2 w[ib\sqrt{\tau}] = -\frac{\partial}{\partial\tau} w[ib\sqrt{\tau}] \tag{35}$$

This function is shown in Fig. 8. When rebinding is not favored (low b), $Y(\tau)$ has a low magnitude and low slope, giving a small but finite probability of rebinding over a long time range. As rebinding becomes more favored (higher b), the magnitude is higher at low values of τ but the slope becomes more negative and at longer times the probability of rebinding is low. At very high values of b, rebinding occurs at very short times after surface dissociation. The integral of $Y(\tau)$ over all time equals one. The molecule always eventually rebinds to the surface.

The surface probability, $S(\tau)$, is plotted in Fig. 9 in terms of the subpopulations $S_1(\tau)$, $S_2(\tau)$, $S_3(\tau)$, and so forth. It is seen that as b becomes larger an increasing number of populations are required to describe the total surface probability. In the case of $b = 0.01$, the total surface probability, $S(\tau)$, may be described as consisting of two populations: those molecules that have not yet been released at time τ, $S_1(\tau)$, and those molecules that were released at time τ_1, rebound at time τ_2, and remained bound at time τ, $S_2(\tau)$. However, for $b = 1$, more populations than $S_1(\tau)$ and $S_2(\tau)$ are required to describe the total surface probability, $S(\tau)$. Here we have calculated the terms $S_2(\tau)$ and $S_3(\tau)$ by numerical integration of Eqs. 32 (with Eq. 35). In the case of $b = \infty$, the expression for each population can be calculated exactly according to Eq. 34. Here it is seen that the 10 first populations, $S_1(\tau)$–$S_{10}(\tau)$, are sufficient to yield $S(\tau)$ for short times τ, but that many more populations are required at longer times τ.

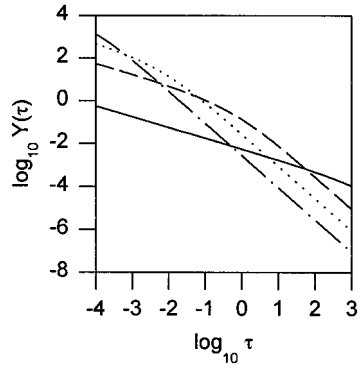

FIGURE 8 Temporal rebinding probability $Y(\tau)$. The function $Y(\tau)$ gives the probability that the molecule rebinds to the surface at time $t = \tau/k_d$, where k_d is the surface dissociation rate, given initial release at time zero. This plot shows $Y(\tau)$ as calculated from Eq. 35 for the rebinding parameter b equal to 0.01 (*line*), 1 (*dash*), 10 (*dot*), and 100 (*dot-dash*).

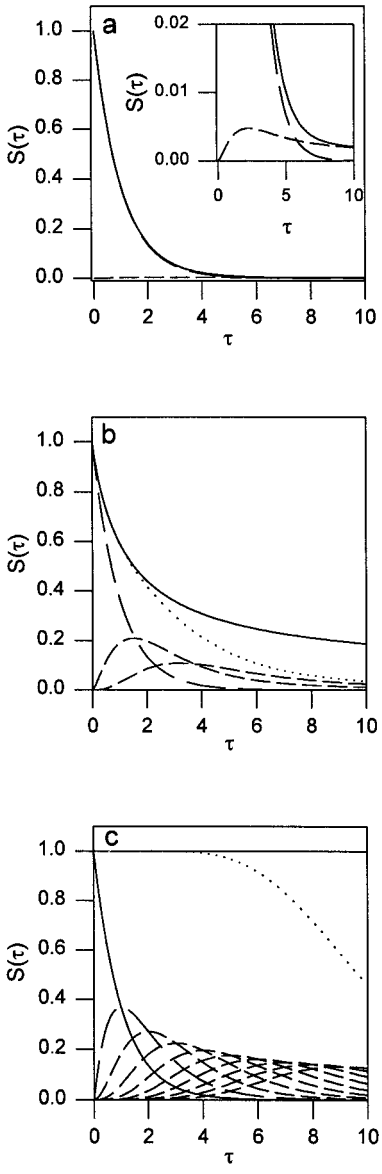

FIGURE 9 Components $S_n(\tau)$ of spatially integrated surface probability. These plots illustrate the manner in which the functions $S_n(\tau)$ sum to give $S(\tau)$ (Eq. 31). Three cases are shown corresponding to (*a*) $b = 0.01$, (*b*) $b = 1$, and (*c*) $b = \infty$. In all three plots, $S(\tau)$ (*line*) was calculated directly from Eq. 29, $S_1(\tau)$ (*long dash*) was calculated from Eq. 32, and $S_2(\tau)$ (*short dash*) was calculated by numerical integration of Eq. 32. In (*a*), the sum of $S_1(\tau)$ and $S_2(\tau)$ is equivalent to $S(\tau)$ within plot resolution. In (*b*), $S_3(\tau)$ (*intermediate dash*) was calculated by numerical integration of Eq. 32. The sum of $S_1(\tau)$, $S_2(\tau)$, and $S_3(\tau)$ (*dot*) is equivalent to $S(\tau)$ only at small times. In (*c*), $S_2(\tau)$–$S_{10}(\tau)$ (*intermediate dash*) were calculated from Eq. 34; the sum of $S_n(\tau)$ (*dot*), for $n = 1$ to 10, is equivalent to $S(\tau)$ only at small times.

Spatial and temporal rebinding probability $W(\rho, \tau)$

The probability density $Q_C(\rho, \tau)$ describes the overall spatial and temporal probability of finding the tagged molecule on the surface following successive rebinding events. Of interest also is the individual probability that the molecule rebinds at a position, ρ, and a later time, τ, given initial release at the origin at time zero. As for $S(\tau)$ and $Y(\tau)$, this individual rebinding probability may be found by first writing the probability density $Q_C(\rho, \tau)$ as the sum of an infinite number of functions

$$Q_C(\rho, \tau) = Q_1(\rho, \tau) + Q_2(\rho, \tau) + Q_3(\rho, \tau) + \cdots \tag{36}$$

where each successive population represents one additional dissociation and rebinding event. Here, $Q_1(\rho, \tau)$ is the probability that the molecule started at position ρ and has not yet dissociated at time τ. $Q_2(\rho, \tau)$ is the probability that the molecule started at position ρ_1, dissociated at time τ_1, rebound at position ρ and time τ_2, and remained bound until time τ; averaged over all possible values of ρ_1, τ_1, and τ_2. $Q_3(\rho, \tau)$ is the probability that the molecule started at position ρ_1, dissociated at time τ_1, rebound at position ρ_2 and time τ_2, dissociated at time τ_3, rebound at position ρ and time τ_4, and remained bound until time τ; averaged over all possible values of ρ_1, ρ_2, τ_1, τ_2, τ_3, and τ_4. Subsequent $Q_n(\rho, \tau)$ functions are found by adding more dissociation and rebinding events.

The first three functions $Q_n(\rho, \tau)$ are

$$\begin{aligned}
Q_1(\rho, \tau) &= \frac{1}{\pi\kappa^2}\exp\left[-\frac{\rho^2}{\kappa^2} - \tau\right] \\
Q_2(\rho, \tau) &= \frac{1}{\pi\kappa^2}\int_0^{\tau} d\tau_2 \int_0^{\tau_2} d\tau_1 \int d^2\rho_1 \\
&\quad \cdot \exp\left[-\frac{\rho_1^2}{\kappa^2} - \tau_1\right] W(|\boldsymbol{\rho} - \boldsymbol{\rho}_1|, \tau_2 - \tau_1)\exp[\tau_2 - \tau] \\
Q_3(\rho, \tau) &= \frac{1}{\pi\kappa^2}\int_0^{\tau} d\tau_4 \int_0^{\tau_4} d\tau_3 \int_0^{\tau_3} d\tau_2 \int_0^{\tau_2} d\tau_1 \\
&\quad \cdot \int d^2\rho_1 \int d^2\rho_2 \exp\left[-\frac{\rho_1^2}{\kappa^2} - \tau_1\right] W(|\boldsymbol{\rho}_2 - \boldsymbol{\rho}_1|, \tau_2 - \tau_1) \\
&\quad \cdot \exp[\tau_2 - \tau_3] W(|\boldsymbol{\rho} - \boldsymbol{\rho}_2|, \tau_4 - \tau_3)\exp[\tau_4 - \tau]
\end{aligned} \tag{37}$$

$W(\rho, \tau)$ is the probability that the molecule rebinds at position ρ and time τ given initial release at the origin at time zero, and the integrals over the ρ_i are over all space. In the limit of no rebinding ($b = 0$), $W(\rho, \tau) = 0$, $Q_n(\rho, \tau) = 0$ for $n \geq 2$, and

$$Q_C(\rho, \tau) = \frac{1}{\pi\kappa^2}\exp\left[-\frac{\rho^2}{\kappa^2} - \tau\right] \tag{38}$$

In the limit of extreme rebinding ($b \to \infty$), $W(\rho, \tau) = \delta(\rho)\,\delta(\tau)$, and

$$\begin{aligned}
Q_2(\rho, \tau) &= \frac{\tau}{\pi\kappa^2}\exp\left[-\frac{\rho^2}{\kappa^2} - \tau\right] \\
Q_3(\rho, \tau) &= \frac{\tau^2}{2!\pi\kappa^2}\exp\left[-\frac{\rho^2}{\kappa^2} - \tau\right] \\
Q_4(\rho, \tau) &= \frac{\tau^3}{3!\pi\kappa^2}\exp\left[-\frac{\rho^2}{\kappa^2} - \tau\right]
\end{aligned}$$

$$Q_C(\rho, \tau) = \frac{1}{\pi\kappa^2}\exp\left[-\frac{\rho^2}{\kappa^2} - \tau\right]\left[1 + \tau + \frac{\tau^2}{2!} + \frac{\tau^3}{3!} + \cdots\right]$$

$$Q_C(\rho, \tau) = \frac{1}{\pi\kappa^2}\exp\left[-\frac{\rho^2}{\kappa^2}\right] \quad (39)$$

These results are consistent with Eqs. 25 and 27.

We are interested in determining the expression for $W(\rho, \tau)$, given the known form for $Q_C(\rho, \tau)$ (Eq. 15). The details of this derivation are given in Appendix B. The simple expression for $W(\rho, \tau)$ is

$$W(\rho, \tau) = \frac{1}{4\pi\tau}\exp\left[-\frac{\rho^2}{4\tau}\right]Y(\tau) \quad (40)$$

where $Y(\tau)$ is given by Eq. 35. $Y(\tau)$ is the probability that a molecule will rebind to the surface at time τ given initial release at time zero. The other factors in Eq. 40 describe the probability that the molecule has traveled a distance ρ in the xy-plane during its time in solution.

$W(\rho, \tau)$ is plotted in Fig. 10 as a function of ρ at various values of b and τ. For all values of τ, the function has a Gaussian shape, centered at $\rho = 0$ with width $(4\tau)^{1/2}$. The peak at $\rho = 0$ decays as $Y(\tau)/(4\pi\tau)$. As rebinding becomes more favored (higher b), the magnitude is higher at lower values of ρ and τ. The slope of $W(\rho, \tau)$ with respect to ρ becomes less negative with longer times, while the slope with respect to τ at smaller values of ρ becomes more negative, so the probability of rebinding at larger values of ρ increases with time τ while the probability of rebinding at smaller values of ρ decreases with τ. The parameter ρ is the distance from the initially bound position, before dissociation, scaled by the parameter γ (Eq. 13). For typical values of the intrinsic dissociation rate k_d and the solution diffusion coefficient D, $\gamma \approx 10$ μm (Fig. 3). Therefore, the abscissa in Fig. 10 represents the approximate size of a cell diameter. The time τ is scaled by k_d (Eq. 14).

DISCUSSION

Understanding the rebinding phenomenon is important not only for understanding the activation of individual cells by soluble ligands but also for understanding the mechanisms by which multicellular structures such as synapses function (Lánská et al., 1994). In addition, the rebinding process is important in measuring receptor-ligand interactions by using the surface plasmon resonance technique (Nieba et al., 1996; O'Shannessy and Winzor, 1996; Schuck and Minton, 1996) and total internal reflection fluorescence microscopy (Thompson et al., 1981; Burghardt and Axelrod, 1981; Thompson, 1982; Thompson and Axelrod, 1983; Pisarchick et al., 1992; Hsieh and Thompson, 1994, 1995; Huang et al., 1994). Rebinding can also play a major role in the performance of surface-based biosensors (Geurts, 1989; Nygren and Stenberg, 1989; Sadana and Madagula, 1994).

We have presented theoretical expressions that describe the process in which ligands dissociate from a surface and then rebind to the surface at the same or a nearby position. Analytical expressions were derived for the spatial and temporal dependence of the probabilities of finding a tagged molecule on the surface (Eq. 15) or in the solution (Eq. 16) given initial placement on the surface. These expressions, and therefore the rebinding phenomenon, depend almost exclusively on the rebinding parameter b (Eq. 19), which depends on the intrinsic association and dissociation rate constants for ligand and receptor, on the density of cell surface receptors, on the concentration of competing ligands in solution, and on the diffusion coefficient of the ligand in solution. The probability density in Eq. 15 was used to derive a simple expression for the probability that a molecule rebinds to the cell surface at a given position and time after initial release at the origin (Eqs. 35 and 40). This probability depends solely on the rebinding parameter b. The analytical results as a group provide fundamental equations that form a basis for subsequent modeling of ligand-receptor interactions in particular geometries.

The theoretical results presented in this paper are related, but not directly comparable, to previous theoretical work. Several papers analytically describe escape and capture probabilities, or the time dependence of binding, for ligands initially placed nearby a spherical cell surface containing receptors that bind the ligands (Berg and Purcell, 1977; DeLisi and Wiegel, 1981; Shoup and Szabo, 1982; Zwan-

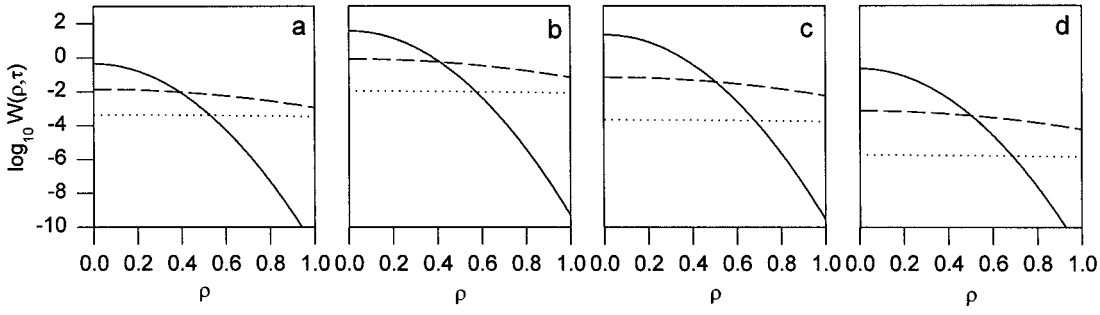

FIGURE 10 Spatial and temporal rebinding probability $W(\rho, \tau)$. The function $W(\rho, \tau)$ gives the probability that the molecule rebinds to the surface at position $r = \rho\gamma$ and time $t = \tau/k_d$, where γ is a characteristic length (Eq. 13) and k_d is the surface dissociation rate, given initial release at the origin at time zero. This plot shows $W(\rho, \tau)$ as calculated from Eq. 40 for (*a*) $b = 0.01$, (*b*) $b = 1$, (*c*) $b = 100$, and (*d*) $b = 10^4$ at values of $\tau = 0.01$ (*line*), $\tau = 0.1$ (*dash*), and $\tau = 1$ (*dot*).

zig, 1990; Goldstein and Dembo, 1995). Our problem differs from these previous studies in that the surface of interest is planar rather than spherical. For a planar surface, the probability that a previously desorbed molecule will rebind to the surface at some later time is unity; i.e., the integral over all time of Eq. 35 is one. As a consequence of the dimension-dependence of the diffusion equation, this result is not the case for a spherical surface. In addition, most of the previous theories are restricted to the case of irreversible ligand-receptor binding. In the limit of irreversible binding ($k_d = 0$ or $k_a = \infty$, with $A = 0$), the rebinding parameter b is infinite (Eq. 19) and, in the theory described here, the molecule never leaves its binding site (Eq. 27). The previous theories for irreversible binding do not have capture probabilities of one not only because the surface is spherical but also because the initial condition is formulated so the ligand is initially placed a finite distance from the surface rather than on a receptor (Eq. 4). A previous work describing reaction at a planar surface (Balgi et al., 1995) differs from the work described here in that the reaction is assumed to be irreversible; dissociation and rebinding are not considered.

The rebinding process has also previously been modeled by using Brownian dynamics simulations. Studies have been carried out both for spherical (Northrup et al., 1986; Northrup, 1988) and planar (Forsten and Lauffenburger, 1994; Lauffenburger et al., 1995) surfaces. Our results are not directly comparable to these studies because, as for previous analytical work, capture probabilities are calculated for irreversible binding and an initial condition placing the ligand a finite distance from the surface. In addition, for the work with planar surfaces, an "effective escape" is defined as the time when a molecule initially crosses a plane a given distance from the surface of interest. However, as shown here (Eq. 15), the molecule will eventually return to the surface and bind.

A different set of previous studies have theoretically described a "reduction of dimensionality" phenomenon in which ligands irreversibly or reversibly bind to specific cell surface receptors by a two-step process involving initial weak, reversible binding to the surface and subsequent diffusion in two dimensions along the surface (Adam and Delbrück, 1968; Wang et al., 1992; Axelrod and Wang, 1994). The theory presented here does not directly address the reduction-of-dimensionality process. Generalization would require a new differential equation for $P_C(r, t)$ (Eq. 2) as well as introduction of a species representing ligands weakly bound to the surface and a different boundary condition for $P_A(r, z, t)$ (Eq. 6).

The theory outlined in this paper can be generalized to ligand-receptor complexes that undergo surface diffusion by including a two-dimensional Laplacian term describing the surface diffusion in the equation for $P_C(r, t)$ (Eq. 2) (Thompson et al., 1981). The theory can also be generalized to surface binding mechanisms that are more complicated than simple bimolecular reactions by fairly straightforward approaches (Hsieh and Thompson, 1994; Huang et al., 1994). To describe mechanisms involving isomerization of the ligand-receptor complexes or bivalent ligand-receptor binding, terms describing the new species are added to the equation for $P_C(r, t)$ (Eq. 2) and differential equations describing the time dependence of the new surface-bound species are added. Previous work suggests that the solution for $P_C(r, t)$ for these mechanisms will be similar to the one shown in Eq. 15, with the major difference being that the characteristic rates α_i are determined by a higher-order polynomial, which depends on the new kinetic rate constants. Each value of α_i appears in a new w function, giving rise to a sum over more than three terms (Eq. 15).

Two methods by which the theoretical results presented in this paper could be experimentally verified are total internal reflection with fluorescence photobleaching recovery (TIR-FPR) (Burghardt and Axelrod, 1981; Pisarchick et al., 1992; Pearce et al., 1992; Hsieh and Thompson, 1995) and total internal reflection with fluorescence correlation spectroscopy (TIR-FCS) (Thompson and Axelrod, 1983). These techniques monitor the kinetic behavior of fluorescently labeled proteins in equilibrium with, and reversibly bound to, planar surfaces. In TIR-FPR, bound proteins are photobleached by a high intensity evanescent field pulse, and subsequent fluorescence recovery is monitored as surface-bound, bleached molecules exchange with unbleached molecules from solution. In TIR-FCS, the fluorescence measured from a small evanescently excited surface area fluctuates with time as individual molecules bind to and dissociate from the surface. The normalized fluorescence fluctuation autocorrelation function contains information about the kinetics of surface association and dissociation.

In the limit of a large observation area where diffusion parallel to the interface (either in solution or on the surface) does not contribute significantly to fluorescence recovery, a straightforward generalization of the theory presented in this work shows that the rate and shape of the TIR-FPR recovery curve is given by Eq. 29 (Thompson et al., 1981). When $k_d \ll k_t$, the data are reaction-limited and are of a single exponential shape with rate k_d. When $k_t \ll k_d$, the data are diffusion-limited and have the shape of a w function with rate k_t. The experimental reaction limit corresponds to the theoretical limit of no rebinding ($b = 0$) and the experimental diffusion limit corresponds to the theoretical limit of significant rebinding ($b \gg 1$). It should be possible to arrange conditions for at least some samples so that they explore the range from the diffusion to the reaction limit with increasing solution concentration (e.g., by choosing a particular solution viscosity or pH). In the diffusion limit, the measured rate k_t should change with the solution concentration A, the diffusion coefficient D, and the site density N as predicted by Eq. 12. In the reaction limit, the measured rate k_d should not change with any of these parameters. Generalizations of the theory described in this paper indicate that TIR-FCS autocorrelation functions also range from reaction-limited to diffusion-limited regimes, with a known analytical dependence of the measured rates on the kinetic association rate k_a, the kinetic dissociation rate k_d, the

solution concentration A, the diffusion coefficient D, and the site density N (Thompson et al., 1981; Thompson, 1982).

In a series of recent and elegant papers, several groups have demonstrated that total internal reflection fluorescence microscopy has the sensitivity necessary to observe single fluorescent molecules as they bind to and dissociate from planar surfaces (Funatsu et al., 1995; Vale et al., 1996; Conibear and Bagshaw, 1996; Xu and Yeung, 1997). This experimental method should allow the rebinding phenomenon to be directly monitored at low surface densities. Here, molecules that dissociate from the surface and rebind would be evident when nearby areas switch from low to high intensity.

APPENDIX A: GENERAL EXPRESSIONS FOR $P_C(r, t)$ AND $P_A(r, z, t)$

The general expression for $P_C(r, t)$ is found by solving Eqs. 2–6 by use of linear transformation theory. The variables x and y are Fourier-transformed to q_x and q_y, z is Laplace-transformed to p, and t is Laplace-transformed to ω. In the subsequent discussion, transformations that have been carried out are denoted solely by the variables q, p, and ω, respectively. One finds that

$$\omega P_C(q, \omega) - [P_C(q, t)]_{t=0} = k_a B[P_A(q, z, \omega)]_{z=0} - k_d P_C(q, \omega) \tag{A1}$$

$$\omega P_A(q, p, \omega) - [P_A(q, p, t)]_{t=0} = D(p^2 - q^2)P_A(q, p, \omega) - Dp[P_A(q, z, \omega)]_{z=0} - D\left[\frac{\partial}{\partial z} P_A(q, z, \omega)\right]_{z=0} \tag{A2}$$

$$D\left[\frac{\partial}{\partial z} P_A(q, z, \omega)\right]_{z=0} = k_a B[P_A(q, z, \omega)]_{z=0} - k_d P_C(q, \omega) \tag{A3}$$

Substitution of the transformed initial conditions (Eqs. 4) gives

$$\omega P_C(q, \omega) - \frac{1}{2\pi}\exp\left[-\frac{q^2a^2}{4}\right] = k_a B[P_A(q, z, \omega)]_{z=0} - k_d P_C(q, \omega) \tag{A4}$$

$$\frac{\omega}{D} P_A(q, p, \omega) = (p^2 - q^2)P_A(q, p, \omega) - p[P_A(q, z, \omega)]_{z=0} - \left[\frac{\partial}{\partial z} P_A(q, z, \omega)\right]_{z=0} \tag{A5}$$

Eq. A5 may be used to obtain a solution for $P_A(q, p, \omega)$ as a function of $[P_A(q, z, \omega)]_{z=0}$ and $\{\partial/\partial z[P_A(q, z, \omega)]\}_{z=0}$. By inverse Laplace transforming ($p \rightarrow z$) the resultant expression and using the boundary condition for $z \rightarrow \infty$ (Eq. 5), one finds that

$$P_A(q, z, \omega) = [P_A(q, z, \omega)]_{z=0}\exp\left[-z\sqrt{\frac{Dq^2 + \omega}{D}}\right] \tag{A6}$$

$$\left[\frac{\partial}{\partial z} P_A(q, z, \omega)\right]_{z=0} = -\sqrt{\frac{Dq^2 + \omega}{D}}[P_A(q, z, \omega)]_{z=0} \tag{A7}$$

Eq. A7 may then be combined with Eq. A3 to give the following solution for $[P_A(q, z, \omega)]_{z=0}$ as a function of $P_C(q, \omega)$:

$$[P_A(q, z, \omega)]_{z=0} = \frac{1}{\sqrt{D}}\frac{k_d P_C(q, \omega)}{\beta + \sqrt{Dq^2 + \omega}} \tag{A8}$$

Eq. A8 may be substituted into Eq. A1 to give an expression for $P_C(q, \omega)$ that is independent of $P_A(q, z, \omega)$:

$$P_C(q, \omega) = \frac{1}{2\pi}\exp\left[\frac{-q^2a^2}{4}\right] \cdot \frac{\beta + \sqrt{Dq^2 + \omega}}{\omega\beta + (\omega + k_d)\sqrt{Dq^2 + \omega}} \tag{A9}$$

where β is defined in Eq. 11. Inverse Laplace transforming ($\omega \rightarrow t$) this expression by defining $\alpha = \omega + Dq^2$ and using the method of partial fractions (Abramowitz and Stegun, 1974) gives a solution for $P_C(q, t)$. Inverse Fourier-transforming ($\mathbf{q} \rightarrow \mathbf{r}$) the result for $P_C(q, t)$ by direct integration finally gives a solution for $P_C(r, t)$ (Eq. 7).

The solution for the probability density, $P_A(r, z, t)$, can be obtained by using Eq. A9 in Eq. A8 and the resultant expression in Eq. A6:

$$P_A(q, z, \omega) = \frac{1}{2\pi}\frac{k_d}{\sqrt{D}}\exp\left[-\frac{z}{\sqrt{D}}\sqrt{Dq^2 + \omega} - \frac{q^2a^2}{4}\right] \cdot \frac{1}{\omega\beta + (\omega + k_d)\sqrt{Dq^2 + \omega}} \tag{A10}$$

The inverse Laplace transform ($\omega \rightarrow t$) of this expression is obtained by defining $\alpha = \omega + Dq^2$ and using the method of partial fractions (see above). The inverse Fourier transform ($\mathbf{q} \rightarrow \mathbf{r}$) is obtained by integration. The result for $P_A(r, z, t)$ is given in Eq. 8.

APPENDIX B: REBINDING PROBABILITIES $Y(\tau)$ AND $W(\rho, \tau)$

The rebinding probability $Y(\tau)$ can be found by Laplace-transforming τ to σ in the expressions for $S_1(\tau)$, $S_2(\tau)$, $S_3(\tau)$, and so forth (Eq. 32). This transformation can be carried out by using the following identities (Abramowitz and Stegun, 1974)

$$L_{\tau\rightarrow\sigma}[\exp(\pm\tau)f(\tau)] = L_{\tau\rightarrow\sigma\mp1}[f(\tau)]$$

$$L_{\tau\rightarrow\sigma}\left[\int_0^\tau f(\tau')d\tau'\right] = \frac{1}{\sigma}L_{\tau\rightarrow\sigma}[f(\tau)]$$

$$L_{\tau\rightarrow\sigma}\left[\int_0^\tau f_1(\tau')f_2(\tau - \tau')d\tau'\right] = L_{\tau\rightarrow\sigma}[f_1(\tau)]L_{\tau\rightarrow\sigma}[f_2(\tau)] \tag{B1}$$

where $f(\tau)$, $f_1(\tau)$ and $f_2(\tau)$ are arbitrary functions. The first three terms are

$$S_1(\sigma) = \frac{1}{1 + \sigma}$$

$$S_2(\sigma) = \frac{Y(\sigma)}{(1 + \sigma)^2} \tag{B2}$$

$$S_3(\sigma) = \frac{Y^2(\sigma)}{(1 + \sigma)^3}$$

Therefore

$$S(\sigma) = \sum_{n=1}^{\infty} S_n(\sigma) = \frac{1}{1+\sigma} \sum_{n=0}^{\infty} \left(\frac{Y(\sigma)}{1+\sigma} \right)^n$$

$$= \left(\frac{1}{1+\sigma} \right) \left(\frac{1}{1 - Y(\sigma)/(1+\sigma)} \right) \tag{B3}$$

$$= \frac{1}{1 + \sigma - Y(\sigma)}$$

The Laplace transform of Eq. 29 is

$$S(\sigma) = \frac{\sqrt{\sigma} + b}{\sigma^{3/2} + b\sigma + \sqrt{\sigma}} \tag{B4}$$

Combining Eqs. B3 and B4 yields

$$Y(\sigma) = \frac{b}{\sqrt{\sigma} + b} \tag{B5}$$

The inverse Laplace transform of Eq. B5 is Eq. 35.

The expression for the probability that a molecule rebinds at position ρ and time τ, given that it dissociated at the origin at time zero, $W(\rho, \tau)$, is derived by Laplace-transforming τ to σ and by Fourier-transforming ρ to c in the expressions for $Q_1(\rho, \tau)$, $Q_2(\rho, \tau)$, $Q_3(\rho, \tau)$, and so forth (Eq. 37). These transformations can be carried out by using the identities shown in Eqs. B1 along with the expression for the Fourier transform of a convolution. The results are

$$Q_1(c, \sigma) = \frac{1}{2\pi} \frac{1}{1+\sigma} \exp\left[-\frac{\kappa^2 c^2}{4} \right]$$

$$Q_2(c, \sigma) = \frac{1}{(1+\sigma)^2} W(c, \sigma) \exp\left[-\frac{\kappa^2 c^2}{4} \right] \tag{B6}$$

$$Q_3(c, \sigma) = \frac{2\pi}{(1+\sigma)^3} W^2(c, \sigma) \exp\left[-\frac{\kappa^2 c^2}{4} \right]$$

Thus

$$Q_C(c, \sigma) = \sum_{n=1}^{\infty} Q_n(c, \sigma)$$

$$= \frac{1}{2\pi} \frac{1}{1+\sigma} \exp\left[-\frac{\kappa^2 c^2}{4} \right] \left\{ \sum_{n=0}^{\infty} \left[\frac{2\pi}{1+\sigma} W(c, \sigma) \right]^n \right\}$$

$$= \frac{1}{2\pi} \frac{1}{1+\sigma} \exp\left[-\frac{\kappa^2 c^2}{4} \right] \tag{B7}$$

$$\cdot \left[\frac{1}{1 - 2\pi W(c, \sigma)/(1+\sigma)} \right]$$

From Eq. A9 with

$$q = \frac{c}{\gamma} \qquad \omega = k_d \sigma \tag{B8}$$

one finds the following expression

$$Q_C(c, \sigma) = \frac{1}{2\pi} \exp\left[-\frac{\kappa^2 c^2}{4} \right] \frac{b + \sqrt{c^2 + \sigma}}{\sigma b + (\sigma + 1)\sqrt{c^2 + \sigma}} \tag{B9}$$

$W(c, \sigma)$ is found by combining Eqs. B7 and B9:

$$W(c, \sigma) = \frac{1}{2\pi} \frac{b}{b + \sqrt{c^2 + \sigma}} \tag{B10}$$

Inverse Laplace-transforming ($\sigma \rightarrow \tau$) Eq. B10 gives

$$W(c, \tau) = \frac{1}{2\pi} \exp[-c^2 \tau] Y(\tau) \tag{B11}$$

where $Y(\tau)$ is given in Eq. 35. Inverse Fourier-transforming ($c \rightarrow \rho$) Eq. B11 gives the expression for $W(\rho, \tau)$ shown in Eq. 40.

This work was supported by National Institutes of Health Grant GM-37145 and National Science Foundation Grant DMB-9024028.

REFERENCES

Abramowitz, M., and I. A. Stegun. 1974. Handbook of Mathematical Functions. Dover Publications, New York. 295ff, 355ff, 1019ff.

Adam, G., and M. Delbrück. 1968. Reduction of dimensionality in biological diffusion processes. *In* Structural Chemistry and Molecular Biology. A. Rich and N. Davison, editors. W. H. Freeman, San Francisco. 198–215.

Axelrod, D., and M. D. Wang. 1994. Reduction-of-dimensionality kinetics at reaction-limited cell surface receptors. *Biophys. J.* 66:588–600.

Balgi, G., D. E. Leckband, and J. M. Nitsche. 1995. Transport effects on the kinetics of protein-surface binding. *Biophys. J.* 68:2251–2260.

Berg, H. C., and E. M. Purcell. 1977. Physics of chemoreception. *Biophys. J.* 20:193–219.

Berg, O., and P. H. von Hippel. 1985. Diffusion-controlled macromolecular interactions. *Annu. Rev. Biophys. Biophys. Chem.* 14:131–160.

Burghardt, T. P., and D. Axelrod. 1981. Total internal reflection/fluorescence photobleaching recovery study of serum albumin adsorption dynamics. *Biophys. J.* 33:455–467.

Conibear, P. B., and C. R. Bagshaw. 1996. Measurement of nucleotide exchange kinetics with isolated synthetic myosin filaments using flash photolysis. *FEBS Lett.* 380:13–16.

DeLisi, C., and F. W. Wiegel. 1981. Effect of nonspecific forces and finite receptor number on rate constants of ligand-cell bound receptor interactions. *Proc. Natl. Acad. Sci. USA.* 78:5569–5572.

Duschl, C., A. Sévin-Landais, and H. Vogel. 1996. Surface engineering: optimization of antigen presentation in self-assembled monolayers. *Biophys. J.* 70:1985–1995.

Erickson, J., B. Goldstein, D. Holowka, and B. Baird. 1987. The effect of receptor density on the forward rate constant for binding of ligands to cell surface receptors. *Biophys. J.* 52:657–662.

Erickson, J. W., R. G. Posner, B. Goldstein, D. Holowka, and B. Baird. 1991. Bivalent ligand dissociation kinetics from receptor-bound immunoglobulin E: evidence for a time-dependent increase in ligand rebinding at the cell surface. *Biochemistry.* 30:2357–2363.

Forsten, K. E., and D. A. Lauffenburger. 1994. Probability of autocrine ligand capture by cell-surface receptors: implications for ligand secretion measurements. *J. Comp. Biol.* 1:15–23.

Funatsu, T., Y. Harada, M. Tokunaga, K. Saito, and T. Yanagida. 1995. Imaging of single fluorescent molecules and individual ATP turnovers by single myosin molecules in aqueous solution. *Nature.* 374:555–559.

Geurts, B. J. 1989. Diffusion limited immunochemical sensing. *Bull. Math. Biol.* 51:359–379.

Goldstein, B., R. G. Posner, D. C. Torney, J. Erickson, D. Holowka, and B. Baird. 1989. Competition between solution and cell surface receptors for

ligand. Dissociation of hapten bound to surface antibody in the presence of solution antibody. *Biophys. J.* 56:955–966.

Goldstein, B., and M. Dembo. 1995. Approximating the effects of diffusion on reversible reactions at the cell surface: ligand-receptor kinetics. *Biophys. J.* 68:1222–1230.

Hsieh, H. V., and N. L. Thompson. 1994. Theory for measuring bivalent surface binding kinetics using total internal reflection with fluorescence photobleaching recovery. *Biophys. J.* 66:898–911.

Hsieh, H. V., and N. L. Thompson. 1995. Dissociation kinetics between a mouse Fc receptor (FcγRII) and IgG: measurement by total internal reflection with fluorescence photobleaching recovery. *Biochemistry.* 34: 12481–12488.

Huang, Z., K. H. Pearce, and N. L. Thompson. 1994. Translational diffusion of bovine prothrombin fragment 1 weakly bound to supported planar membranes: measurement by total internal reflection with fluorescence pattern photobleaching recovery. *Biophys. J.* 67:1754–1766.

Lánská, V., P. Lánský, and C. E. Smith. 1994. Synaptic transmission in a diffusion model for neural activity. *J. Theor. Biol.* 166:393–406.

Lauffenburger, D. A., K. E. Forsten, B. Will, and H. S. Wiley. 1995. Molecular/cell engineering approach to autocrine ligand control of cell function. *Ann. Biomed. Eng.* 23:208–215.

Lookene, A., O. Chevreuil, P. Østergaard, and G. Olivecrona. 1996. Interaction of lipoprotein lipase with heparin fragments and with heparin sulfate: stoichiometry, stabilization, and kinetics. *Biochemistry.* 35: 12155–12163.

Model, M. A., and G. M. Omann. 1995. Ligand-receptor interaction rates in the presence of convective mass transport. *Biophys. J.* 69:1712–1720.

Nieba, L., A. Krebber, and A. Plückthun. 1996. Competition BIAcore for measuring true affinities: large differences from values determined from binding kinetics. *Anal. Biochem.* 234:155–165.

Northrup, S. H. 1988. Diffusion-controlled ligand binding to multiple competing cell-bound receptors. *J. Phys. Chem.* 92:5847–5850.

Northrup, S. H., M. S. Curvin, S. A. Allison, and J. A. McCammon. 1986. Optimization of Brownian dynamics methods for diffusion-influenced rate constant calculations. *J. Chem. Phys.* 84:2196–2203.

Nygren, H., and M. Stenberg. 1989. Immunochemistry at interfaces. *Immunology.* 66:321–327.

O'Shannessy, D. J., and D. J. Winzor. 1996. Interpretation of deviations from pseudo-first-order kinetic behavior in the characterization of ligand binding by biosensor technology. *Anal. Biochem.* 236:275–283.

Otis, T. S., Y. Wu, and L. O. Trussell. 1996. Delayed clearance of transmitter and the role of glutamate transporters at synapses with multiple release sites. *J. Neurosci.* 16:1634–1644.

Pearce, K. H., R. G. Hiskey, and N. L. Thompson. 1992. Surface binding kinetics of prothrombin fragment 1 on planar membranes measured by total internal reflection fluorescence microscopy. *Biochemistry.* 31: 5983–5995.

Pisarchick, M. L., D. Gesty, and N. L. Thompson. 1992. Binding kinetics of an anti-dinitrophenyl monoclonal Fab on supported phospholipid monolayers measured by total internal reflection with fluorescence photobleaching recovery. *Biophys. J.* 63:215–223.

Sadana, A., and A. Madagula. 1994. A fractal analysis of external diffusion-limited first-order kinetics for the binding of antigen by immobilized antibody. *Biosens. Bioelectr.* 9:45–55.

Schuck, P., and A. P. Minton. 1996. Analysis of mass transport-limited binding kinetics in evanescent wave biosensors. *Anal. Biochem.* 240: 262–272.

Shoup, D., and A. Szabo. 1982. Role of diffusion in ligand binding to macromolecules and cell-bound receptors. *Biophys. J.* 40:33–39.

Thompson, N. L. 1982. Surface binding rates of nonfluorescent molecules may be obtained by total internal reflection with fluorescence correlation spectroscopy. *Biophys. J.* 38:327–329.

Thompson, N. L., and D. Axelrod. 1983. Immunoglobulin surface binding kinetics studied by total internal reflection with fluorescence correlation spectroscopy. *Biophys. J.* 43:103–114.

Thompson, N. L., T. P. Burghardt, and D. Axelrod. 1981. Measuring surface dynamics of biomolecules by total internal reflection fluorescence with photobleaching recovery or correlation spectroscopy. *Biophys. J.* 33:435–454.

Vale, R. D., T. Funatsu, D. W. Pierce, L. Romberg, Y. Harada, and T. Yanagida. 1996. Direct observation of single kinesin molecules moving along microtubules. *Nature.* 380:451–453.

Wang, D., S. Gou, and D. Axelrod. 1992. Reaction rate enhancement by surface diffusion of adsorbates. *Biophys. Chem.* 43:117–137.

Xu, X. H., and E. S. Yeung. 1997. Direct measurement of single-molecule diffusion and photodecomposition in free solution. *Science.* 275: 1106–1109.

Zwanzig, R. 1990. Diffusion-controlled ligand binding to spheres partially covered by receptors: an effective medium treatment. *Proc. Natl. Acad. Sci. USA.* 87:5856–5857.